Geotechnical and Geophysical Site Characterisation 5 – Lehane, Acosta-Martínez & Kelly (Eds)

Field measurements of the variability in shear strain and pore pressure generation in Christchurch soils

J.N. Roberts, K.H. Stokoe, S. Hwang, B.R. Cox, Y. Wang, & F.M. Menq
The University of Texas at Austin, Austin, Texas, U.S.A.

S. van Ballegooy
Tonkin & Taylor Ltd, Auckland, New Zealand

ABSTRACT: A significant problem continually facing geotechnical engineers is predicting the likelihood of pore-water pressure generation leading to liquefaction triggering of soils in future earthquakes. These soils include granular soils ranging from gravels to sands to silts in saturated and nearly-saturated conditions. The problem for geotechnical engineers is that their predictions are normally based on simplified empirical correlations. A direct, in-situ test method has been developed to: (1) investigate the shear strain at which pore pressure generation begins, (2) investigate the combined effects of shear strain amplitude and number of loading cycles on pore pressure generation, and (3) estimate the point at which liquefaction "triggering" occurs. The field test involves staged, controlled shaking at the ground surface with a large vibroseis and monitoring ground motions and pore pressures over a range in depths with an embedded array of push-in sensors. In this paper, results from testing several soil types that were subjected to the 2010-2011 Canterbury Earthquake Sequence are presented. Responses to the controlled shaking vary from significant positive pore pressure generation (contraction) to negative pore pressure generation (dilation). The impacts of soil type, soil density, and saturation level on these responses are discussed and the complex field behavior is shown.

1 INTRODUCTION

The 2010-2011 Canterbury Earthquake Sequence (CES) caused repeated, widespread liquefaction of the natural soil in and around Christchurch, New Zealand. The resulting soil liquefaction was responsible for an estimated one-third of the damage to the city and its infrastructure, which is costing insurers upwards of $40 billion NZD in the effort to rebuild the city.

In an attempt to mitigate the risk of liquefaction triggering in future earthquakes, large-scale testing of various shallow ground improvement methods for residential structures and low-rise buildings was undertaken by Tonkin & Taylor Ltd on behalf of the New Zealand Earthquake Commission (EQC). Within the framework of this ground-improvement project, researchers from The University of Texas at Austin (UT) performed: (1) pre-shaking characterization of each test location with small-strain, crosshole seismic tests and (2) large-scale, staged shaking tests of the natural and ground-improved soils to study liquefaction triggering. The staged, shaking tests were performed with a large vibroseis named T-Rex as shown in Figure 1a. The objective of the shaking tests was to simulate a wide range of earthquake-loading conditions in situ while monitoring the resulting ground motions and generation of excess pore-water pressures at depth with an embedded array of push-in sensors.

The testing technique and the effectiveness of ground improvements to inhibit liquefaction triggering have been discussed in past publications (Stokoe et al, 2014, and van Ballegooy et al, 2015). The focus of this paper is on the variability in pore pressure responses measured in natural soils at Site 6, one of three test sites that were selected in the Christchurch suburbs for the liquefaction-triggering study. The observed variability at Site 6 is attributed to differences in: (1) soil type, (2) soil density, and (3) degree of saturation as discussed below.

2 OVERVIEW OF TESTING TECHNIQUES

2.1 *Small-strain crosshole testing*

Small-strain seismic testing using the crosshole method was performed to initially characterize the states of the natural soil and ground improvements prior to large-scale shake testing with T-Rex. The constrained compression wave velocity, V_P, and shear wave velocity, V_S, were measured at 20-cm depth intervals from depths of 0.6 to 5.0 m. The velocity profiles as a function of depth provided an

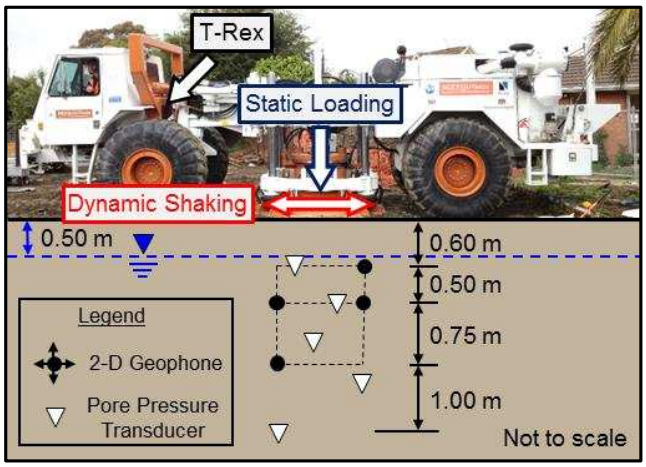

(a) Cross-sectional perspective of T-Rex and embedded array of sensors during shaking

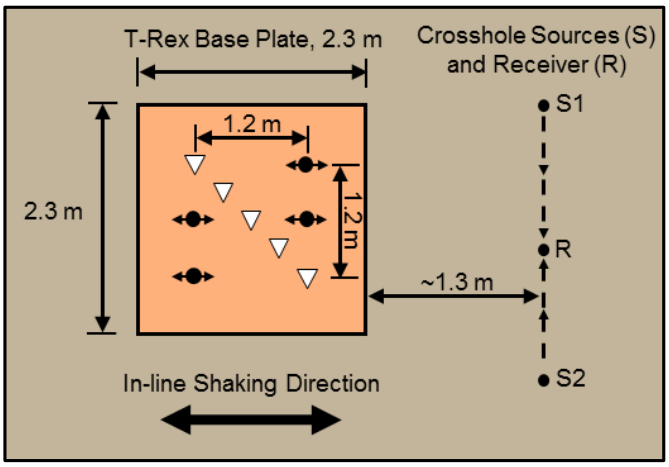

(b) Plan view of the T-Rex baseplate, embedded array of sensors, and approximate location of crosshole seismic testing

Figure 1. Cross-sectional and plan views of in-situ shaking tests with T-Rex at Site 6

initial characterization of the zone of interest. The crosshole testing was performed by pushing two source rods on either end of a linear array and a receiver rod with a bottom 3-D geophone in the middle of the array. The horizontal distance between the source rods (denoted as S1 and S2 in Figure 1b) varied somewhat but was about 2.5 m. Also, one of the two travel paths included the ground-improved zone when present. More information on this testing can be found in Stokoe et al, 2014.

The V_P measurements were used to locate the depth below the ground surface at which 100 % saturation existed. At Site 6, the ground water table was approximately 0.5 m below the ground surface. The depth to 100 % saturation varied around the site but was approximately 1.5 m for the two natural-soil sites. Complete saturation was easily identified by a high-frequency, wave arrival in the time record and a corresponding V_P ranging from about 1,450 to 1,700 m/s.

Measurement of V_S was used to evaluate the shear stiffness of the soil skeleton. The small-strain shear modulus, G_{max}, was calculated from the mass density, ρ, and V_S ($G_{max} = \rho V_S^2$). Where noted, the measured V_S was also stress-corrected to account for the increased confining pressure during shake testing that results from the distribution of the weight of T-Rex (26.7 kN (60,000 lbs)) through the baseplate.

2.2 *In-situ shake testing with T-Rex*

The coupled behavior of shear strain and generation of excess pore water pressure over a large range of strains was evaluated by controlled, horizontal shaking at the ground surface with T-Rex and monitoring the soil response at shallow depths with an embedded array of ground motion and pore pressure sensors (see Figure 1a). Besides shaking, T-Rex was also used to install all embedded sensors using the pushing mechanism at the rear of the machine. Four, 2-dimensional velocity transducers (2-D geophones) and five, pore-water pressure transducers (PPTs) were installed within the plan dimensions of the baseplate of T-Rex at depths ranging from 0.60 to 2.90 m. The location of T-Rex and the embedded sensors during shaking are shown in cross-section in Figure 1a and in plan view in Figure 1b. The relative location of the pre-shaking, crosshole testing array is also shown in Figure 1b.

2.3 *Resonant column testing of reconstituted sand specimens*

Torsional resonant column (RC) testing was performed at UT on reconstituted fine-sand specimens from one depth (1.2 m) at the first, natural-soil test panel (6-NS-1) and two depths (2.0 and 3.0 m) at the second, natural-soil test panel (6-NS-2). The RC testing was used to investigate the dynamic properties of the sand over a shear strain range of 0.00002 to 0.1 %. The RC test had a fixed-free configuration with the top of the specimen free. The top of the specimen was excited with torsional motion and a dynamic response curve was determined from which V_S, shear modulus, G, and shear strain, γ, were determined. More information on the RC testing for this project can be found in Wang (2015).

3 SUBSURFACE CONDITIONS AT THREE TEST PANELS

The dynamic performance evaluated at three test panels at Site 6 are presented below. Two natural soil test panels (6-NS-1 and 6-NS-2) and one test panel improved by the Rapid Impact Compaction method (6-RIC-1) are discussed. The 6-RIC-1 test panel is included because it provides insight into the behavior of naturally-occurring Christchurch sands in a denser state. The RIC ground improvement method is illustrated in Figure 2.

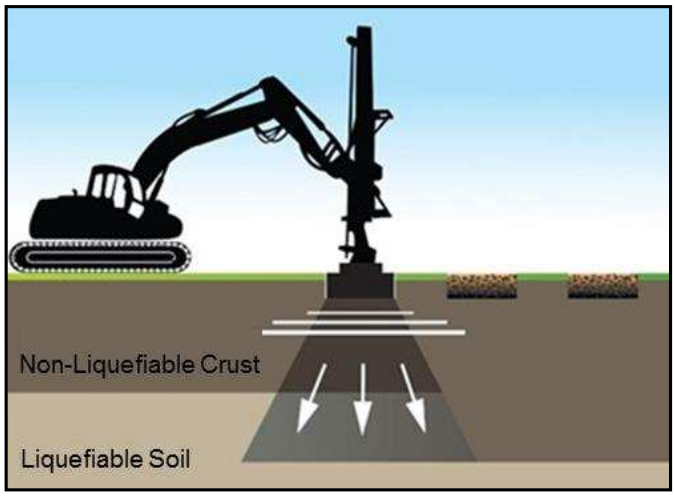

Figure 2. Rapid Impact Compaction (RIC) method used to densify natural silty sand at Site 6

A detailed soil profile at each test panel was determined after shake testing by dewatering the test panel, trenching along the centerline to a depth generally less than 3.5 m, logging and photographing the trench wall, and recovering disturbed samples for laboratory testing. The soil profile varied somewhat from panel to panel but can generally be described by a simplified, four-layer profile as:

Layer 1 – fine to medium sand with some silt and organics (thickness ~0.7 m),
Layer 2 – silt with trace organics; non-plastic, stiff (thickness ~0.45 m),
Layer 3 – sandy silt; non-plastic, stiff (thickness ~0.35 m), and
Layer 4 – silty fine sand, loose to medium dense; reducing silt component with depth (extending beyond 5 m based on borings).

4 RESULTS FROM CONTROLLED SHAKING OF THREE TEST PANELS WITH T-REX

The cyclic loading applied during shake testing at each test panel was: (1) staged, horizontal loading applied at the ground surface, (2) sinusoidal loading applied at 10 Hz for 100 cycles (N), and (3) loading performed in five distinct stages that nominally ranged from the lowest level (± 13 kN) to the highest level (± 107 or 133 kN).

4.1 *Excess pore pressure ratio and shear strain*

The pore pressure measured by the five PPTs is expressed in terms of an excess pore pressure ratio, r_u. This ratio is defined as the excess pore pressure, Δu, divided by the initial vertical effective stress, σ_v'. The value of σ_v' includes a component from the hold-down force applied by T-Rex. In this study, liquefaction triggering is predicted to occur by extrapolating the r_u-logγ curve to 100 %.

The four, 2-D geophones were used to measure particle velocities in the soil at various depths during cyclic loading. By integrating the velocity-time records with respect to time, displacement-time records were determined which were, in turn, used to evaluate shear strain at any location within the instrumented array using the 4-node, displacement-based, shear-strain calculation method presented by Cox et al, 2009. Example r_u-time and γ-time records for the largest level of shaking at one natural-soil test panel (6-NS-1) from depths 0.60 and 2.10 m are presented in Figures 3 and 4, respectively.

The r_u-time records from two depths show some of the natural variability in the coupled r_u-γ response of the soil. At 0.60 m, the shear strain is large (0.6 %), the soil is unsaturated (Sr < 99 %) even though it is below the water table, and r_u only increases to about 27 % after 100 cycles. However, r_u continues to increase after the end of shaking, indicating that there are areas of higher pore pressures in the vicinity that are dissipating in the direction of this shallow PPT (Figure 3a). In contrast, at 2.10 m, the shear strain is significant but smaller (0.14 %), the soil is saturated (Sr = 100 %), and r_u increases to about the same level after 100 cycles as at 0.6 m. However, r_u begins rapidly dissipating at the end of shaking (Figure 4a). Besides the complexity in pore pressure at 0.6 m, the difference in dissipation rate is related to the permeability of the soil, which is reflected in soil type. The fines content of the soil at 0.60 m ranges from 80 to 96 % while the soil at 2.10 m has a fines content ranging from 1 to 5 % based on laboratory testing. In comparison to lower-permeability silty soil, the rapid dissipation of r_u seen in Figure 4a is expected at that depth for a sand with few fines.

4.2 *Cyclic stress ratio (CSR) at a given number of cycles of loading (N)*

The cyclic stress ratio presented herein is the CSR at a given number of cycles, N, and is defined as the cyclic shear stress, τ, divided by the vertical effective stress, σ_v', at N. The vertical total stress is calculated using unit weights of 17 kN/m^3 and 19.5 kN/m^3 for soils above and below the water table, respectively. These unit weights are estimated from partially- and fully-saturated unit weights of the reconstituted laboratory specimens from the 6-NS-1 and 6-NS-2 test panels with similar laboratory and field V_S values. The vertical total stress, σ_v, also includes a component from the hold-down force applied by T-Rex, which is calculated using Poulos & Davis (1974) stress distribution equations for a square surface footing (i.e. the 2.3- by 2.3-m baseplate of T-Rex). At low levels of shaking when no excess pore-water pressure is generated, σ_v' is simply σ_v minus the static pore pressure. At larger levels of shaking when excess pore pressure is generated, the vertical effective stress

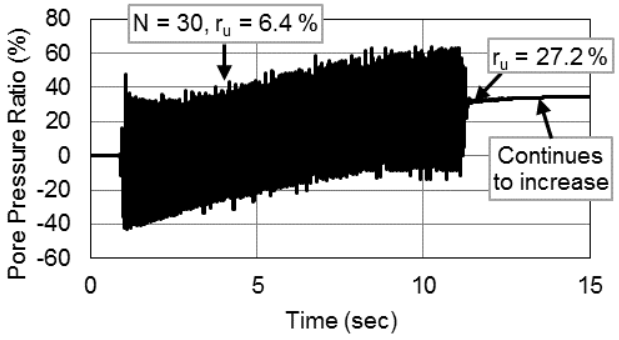

(a) Variation of excess pore pressure ratio (r_u) with time of shaking

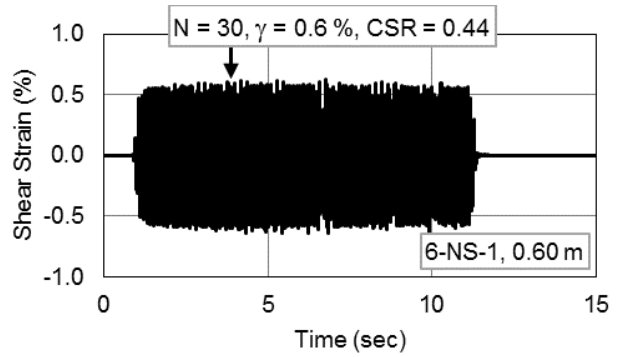

(b) Variation of shear strain (γ) with time of shaking

Figure 3. Variations in r_u and γ with time of shaking at a depth of 0.6 m at the natural soil test panel, 6-NS-1; frequency = 10 Hz; values of r_u, γ, and CSR at N = 30 cycles are identified.

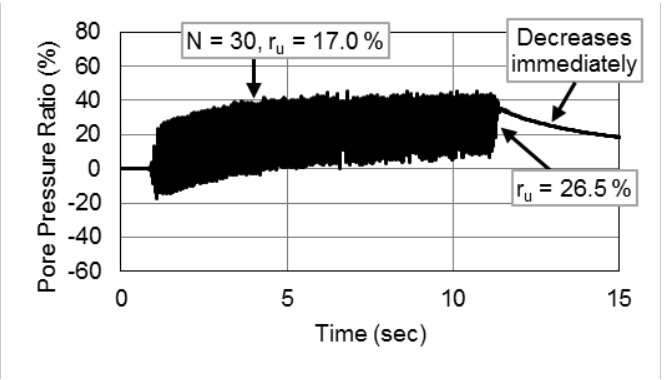

(a) Variation of excess pore pressure ratio (r_u) with time of shaking

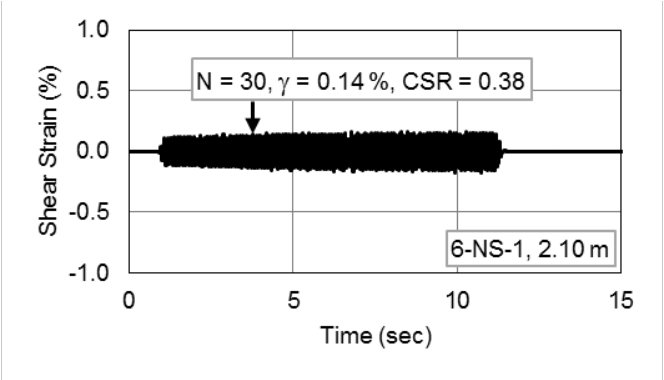

(b) Variation of shear strain (γ) with time of shaking

Figure 4. Variations in r_u and γ with time of shaking at a depth of 2.1 m at the natural soil test panel, 6-NS-1; frequency = 10 Hz; values of r_u, γ, and CSR at N = 30 cycles are identified.

is adjusted according to the excess pore pressure measured by the PPTs.

The CSR at a given N (CSR_N) is determined from the cyclic shear strain at N (γ_N calculated from shake testing), the initial shear modulus at the start of shaking (G_{max} calculated from crosshole testing and adjusted for the static load of T-Rex), the value of G_{max} adjusted for the change in σ_v' due to the generation of r_u at N (denoted as $G_{max,ru}$), and the normalized shear modulus reduction curve, G/G_{max}-logγ, determined from RC testing at the initial σ_v' that is now adjusted for σ_v' at N by using $G_{max,ru}$. By multiplying $G_{max,ru}$ times the original G/G_{max}-logγ curve, a G-logγ curve adjusted for the increased pore pressure (r_u) is constructed. The value of G at the increased pore pressure and γ_N is calculated (denoted as $G_{\gamma N,ru}$). This calculation can be expressed as:

$$CSR_N = \frac{\tau}{(\sigma_v')_N} = \frac{\gamma_N \times G_{max,ru} \times (G/G_{max})_{\gamma N}}{(\sigma_v')_N} \quad (1)$$

in which the right-hand side simply equals $\gamma_N \times G_{\gamma N,ru} / (\sigma_v')_N$. The equation for the shear modulus reduction curve from RC testing utilizes the modified hyperbolic equation as defined by:

$$\frac{G}{G_{max}} = \frac{1}{1+\left(\frac{\gamma}{\gamma_r}\right)^a} = \frac{1}{1+\left(\frac{\gamma}{0.038\,\%}\right)^{0.80}} \quad (2)$$

where "a" is the curvature coefficient and γ_r equals γ at G/G_{max} = 0.5. The values of "a" and γ_r in Equation 3 were determined with SP sand from natural soil test panel 6-NS-2 at a confining pressure of about 0.25 atmospheres (Wang, 2015). Work on determining CSR at increasing strain levels during generation of r_u is continuing.

4.3 *General trends in the r_u-logγ relationship*

4.3.1 *Variation in r_u-logγ with N, V_S, and density*

The behavior that leads to liquefaction triggering is best understood in terms of the r_u-logγ relationship at a selected number of loading cycles (N). The variation in pore pressure generation measured during shake testing can often be explained by one or more of the following: 1) degree of saturation, 2) relative density, and 3) soil type. To remove one source of variability, all soils selected for additional comparisons hereafter are 100 % saturated, with V_P > 1,450 m/s. In Table 1, the locations, characteristics, stress-corrected V_S (V_S*) for the load of T-Rex, and Unified Soil Classification System (USCS) symbol of each soil "layer" are listed.

In Figures 5 and 6, the results corresponding to the deepest PPT at the 6-NS-1, 6-NS-2, and 6-RIC-1 test panels are shown for 10 and 30 cycles, respectively. The soil at these locations have been identified as

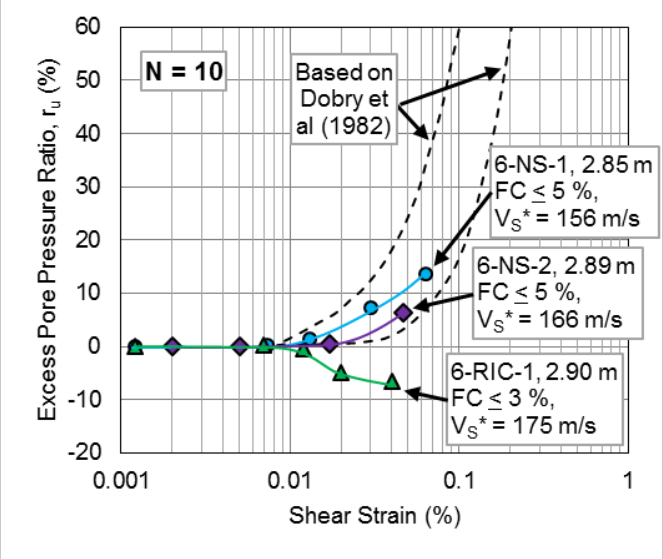

Figure 5. Variation in r_u with γ and V_S ("density") at N = 10 cycles for SP material

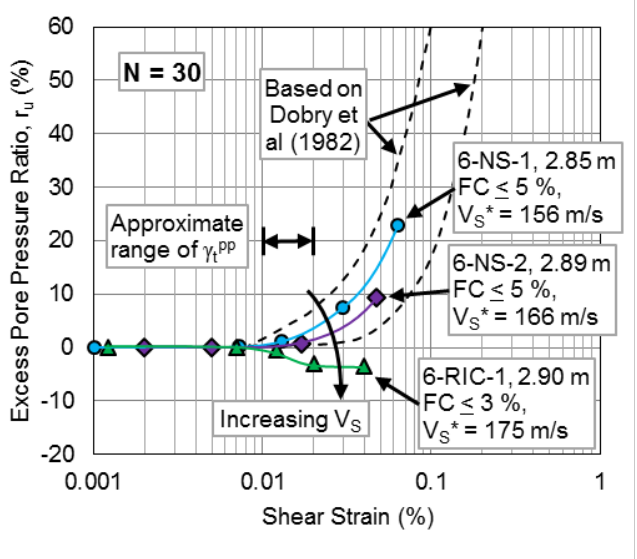

Figure 6. Variation in r_u with γ and V_S ("density") at N = 30 cycles for SP material

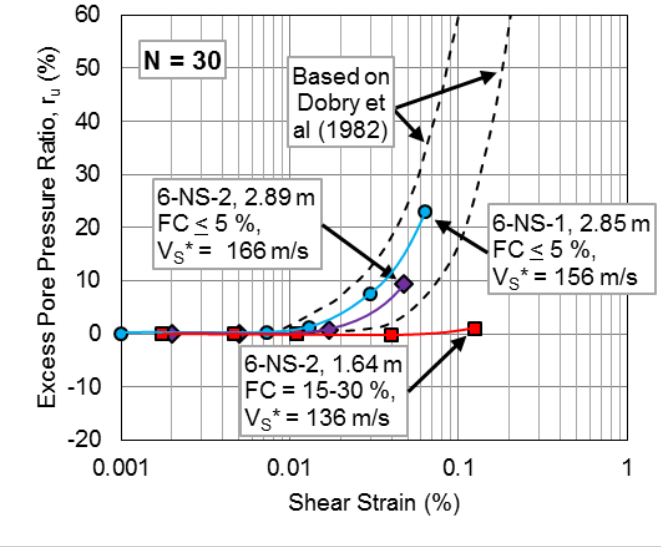

Figure 7. Effect of fines content on r_u-logγ relationships

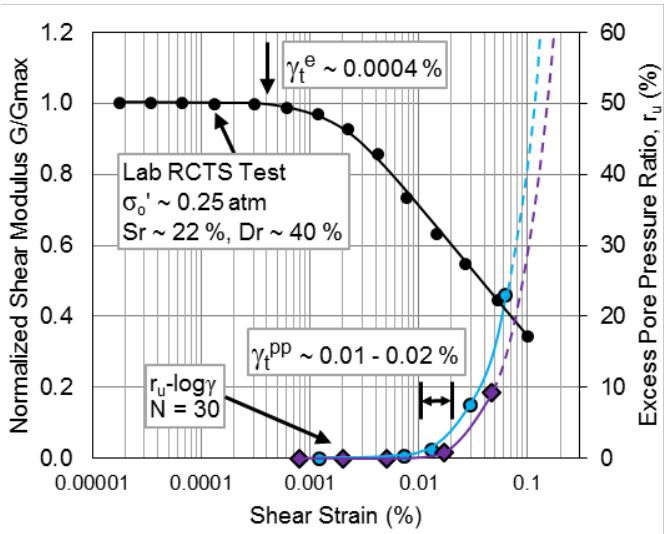

Figure 8. Comparison between the G/G_{max}-logγ curve from RC testing and the r_u-logγ relationships at test panels 6-NS-1 and 6-NS-2

poorly graded sands with less than 5 % fines content. The results for the loose, liquefiable sands from the two natural soil test panels fall within the dashed zone that designates the r_u-logγ behavior of liquefiable soils based on laboratory results analyzed by Dobry et al (1982). The denser natural soil at the 6-RIC-1 test panel, however, generates negative excess pore pressures and clearly falls outside the zone for liquefiable soils.

The number of cycles selected for this analysis has little effect on the conclusions drawn from the results. Despite the increase in pore pressure observed from 10 to 30 cycles at the two natural soil test panels, the r_u-logγ relationships still fall well within the zone for liquefiable soils. At the 6-RIC-1 test panel, the excess pore pressure is slightly less negative after 30 cycles than at 10 cycles but it is still well outside the dashed zone; hence, no liquefaction. Investigation of the effect of N is ongoing and the remainder of the discussion focuses on other effects at N = 30 cycles.

Table 1. Locations and characteristics of saturated soils compared in Figures 5 though 8

Test Panel	Depth	FC min.	FC max.	σ_v'*	V_P	V_S	V_S*	USCS
	m	%	%	(kPa)	m/s	m/s	m/s	
6-NS-1	2.85	1	5	27.0	1,728	146	156	SP
6-NS-2	1.64	15	30	27.0	1,473	113	136	SM
6-NS-2	2.89	1	5	27.2	1,676	155	166	SP
6-RIC-1	2.90	1	3	27.2	1,607	164	175	SP

*Stress-corrected for the weight of T-Rex during shake testing

It is seen in Figure 6 that, as V_S increases, the tendency to generate positive values of r_u decreases. In this case, V_S is simply a surrogate for density or relative density. Based on the RC testing of Wang (2015), the V_S values indicate relative densities are estimated to be on the order of 40, 55, and 80 % for the 6-NS-1, 6-NS-2, and 6-RIC-1 test panels,

respectively, in the depth range of 2.85 to 2.90 m. Furthermore, the threshold strain at which r_u begins to be generated, γ_t^{pp}, is in the range of 0.01 to 0.02 %, with γ_t^{pp} increasing as V_S increases. However, investigation of γ_t^{pp} is readily performed in these measurements in-situ and is continuing.

4.3.2 *Variation in r_u-logγ with fines content*

The effect of soil type expressed in terms of fines content is observed in Figure 7 where the results of a silty sand with fines content ranging from 15 to 30 % from a depth 1.64 m at 6-NS- 2 is compared with the results of the clean sands from depths of 2.85 m at 6-NS-1 and 2.89 m at 6-NS-2. Despite being fully saturated and having a lower stiffness than the clean sands as indicated by the V_S (136 m/s versus 156 and 166 m/s, respectively), the silty sand generates very little excess pore pressure (r_u = 1.1 %) even at a relatively high level of shear strain ($\gamma \sim 0.12$ %).

4.3.3 *Normalized shear modulus reduction curve and threshold strains*

The elastic threshold strain, γ_t^e, the nonlinearity in the G/G_{max}-logγ relationship and the threshold strain at which excess pore pressure generation begins, γ_t^{pp}, can be compared in these liquefiable sands (SP) be combining the results of shake testing and RC testing. The normalized shear modulus reduction curve from RC testing is shown in Figure 8 for a reconstituted specimen taken from 6-NS-2 at a depth of 2.0 m. The specimen has a fines content of 2 % and a $D_r \sim 40$ %. The value of γ_t^e marks the boundary between the linear and nonlinear-elastic shear strain ranges. The r_u-logγ relationships in Figure 8 come from the shake testing results from depths 2.85 and 2.90 m at test panels 6-NS-1 and 6-NS-2, respectively. These sands have a fines content ranging from 1 to 5 %. The range in the values of γ_t^{pp} delineates the boundary between the nonlinear-inelastic strain range and the strain range where volume change begins.

The pore pressure threshold strains in the range of 0.01 to 0.02 % in Figure 8 match well with values reported in the literature for liquefiable sands from both laboratory and field testing (e.g. Dobry et al, 1982, Cox et al, 2009, Roberts, 2014). The range in values of γ_t^{pp} corresponds to strains at which values of G/Gmax are in the range of 0.7 to 0.6 for this sand, indicating that the soil has already lost 30 to 40 % of its initial stiffness before volume change, hence r_u, begins to occur.

5 CONCLUSIONS

Staged, controlled shaking with T-Rex of three, instrumented test panels of natural soils was performed to investigate in-situ the r_u-logγ relationships leading to possible liquefaction. The primary conclusions from this study are as follows.

1. Significant variability in the r_u-logγ relationships was measured due to degree of saturation, density (reflected in the V_S values), and fines content (SP versus SM soils).
2. Loose, clean sand with FC $\leq$ 5 % (SP and D_r ~40 to 55 %) generated a positive r_u-logγ relationship that would predict liquefaction.
3. The threshold strain at which pore pressure generation began, γ_t^{pp}, for the loose, clean sands was in the range of 0.01 to 0.02 %.
4. Denser, clean sand with FC $\leq$ 5 % (SP and $D_r \sim$ 80 %) generated a negaitve r_u-logγ relationship that would predict no liquefaction.
5. Loose, silty sand with FC = 15 – 30 % (SM) generated little to no r_u at $\gamma \leq 0.12$ %.
6. The range of γ_t^{pp} of the loose, clean sands was about 25 to 50 times the γ_t^e of the G/G_{max}-logγ relationship and was in the nonlinear range where G/G_{max} was in the range of 0.7 to 0.6.

6 ACKNOWLEDGEMENTS

Financial support for this study was provided through the National Science Foundation under grants from the: RAPID Program (CMMI-0343524), NEES Program (CMMI-0927178), and Graduate Fellowship Program (DGE-1110007). Other financial support was received from the New Zealand Earthquake Commission (EQC). This support is gratefully acknowledged.

7 REFERENCES

Cox, B.R., Stokoe, K.H., and Rathje, E.M. 2009. An In Situ Test Method for Evaluating the Coupled Pore Pressure Generation and Nonlinear Shear Modulus Behavior of Liquefiable Soils. *ASTM Geotech. Testing J.*, Vol. 32(1).

Dobry, R., Ladd, R.S., Yokel, F.Y., Chung, R.M., and Powell, D. 1982. *Prediction of Pore Water Pressure Buildup and Liquefaction of Sands during Earthquakes by the Cyclic Strain Method*. Washington, D.C.: National Bureau of Standards.

Poulos, H.G., and Davis, E.H. 1974. *Elastic Solutions for Soil and Rock Mechanics*. Univ. of Sydney.

Roberts, J.N. 2014. *Direct In-Situ Evaluation of Liquefaction Suscept*. M.S. thesis. UT Austin.

Stokoe, K., Roberts, J., Hwang, S., Cox, B., Menq, F., & van Ballegooy, S. 2014. Effectiveness of Inhibiting Liquef. Triggering by Shallow Ground Imprvmnt Methods: Initial Field Shaking Trials with T-Rex. In Orense, Towhata, & Chouw (Eds.), *Soil Liquefaction During Recent Large-Scale Earthquakes* (pp. 193-202). London: Taylor & Francis Group.

van Ballegooy, S., Roberts, J.N., Stokoe, K.H., Cox, B.R., Wentz, F.J., Hwang, S. 2015. Large-Scale Testing of Shallow Ground Improvements using Controlled Staged-Loading with T-Rex. *Proc. 6th Inter. Conf. on Earthquake Geotech Engrg, November.* Christchurch, New Zealand.

Wang, Y. 2015. *Dynamic Properties of Fine Liquefiable Sand and Calcareous Sand from Resonant Col. Testing*. M.S. thesis. UT Austin.